Chapter 7
Geological and Geotechnical Studies of Nungkao Landslide Along Imphal-Jiribam National Highway, NH-37, Manipur, India

Kh. Mohon Singh and M. Okendro

Abstract Landslide on a mountainous stretch of the National Highway is a serious concern because they hinder traffic. Anthropogenic activities in the large-scale excavation of the natural slope to expand the existing national highway can significantly alter the slope mass sliding properties. The present study examines the rock mass current geotechnical state and the locations of potential failures in the Imphal Jiribum national highway of (NH-37) in Manipur. Rock mass characterizations and uniaxial compression strength tests have been carried out for the entire study area. According to kinematic analysis and field observations, the study result reveals that the Nungkao landslide is unstable. Wedge collapses are dominant. The factor of safety for rock wedge failure mode has indicated stable conditions. Based on the plasticity index chart, soil samples collected from the site have lower moisture content, which indicates that the soil is of an inorganic origin. The negative (−ve) value of the liquidity index (−1.18) and the positive (+ve) value of the consistency index (3.03) infer that the slope materials remain in the solid-state or semi-solid state, which indicates the slope is stable. Safety factor calculation also shows stable soil slope conditions. However, frequent slides still occur in the area. Effective preventive measures are suggested to improve slope stability accordingly.

Keywords Slope mass rating (SMR) · Kinematic analysis · Uniaxial compressive strength (UCS) · Factors of safety · Nungkao—Manipur

7.1 Introduction

Landslide generally occurs in mountainous and hilly areas with thick or thin soil and/ or weathered rocks. It is a common natural hazard in the hilly terrain of Manipur, causing immense threats to life, extensive losses, and environmental problems. Despite advances in science and technology, economic and societal losses due

Kh. Mohon Singh (✉) · M. Okendro
Department of Geology, Imphal College, Imphal 795001, Manipur, India
e-mail: khuraijammohonsingh98@gmail.com

© The Author(s), under exclusive license to Springer Nature Switzerland AG 2023

P. Thambidurai and T. N. Singh (eds.), *Landslides: Detection, Prediction and Monitoring*,
https://doi.org/10.1007/978-3-031-23859-8_7

to landslides are still a major concern in the public domain. The study area is an integral part of the mobile belt of the Indo-Myanmar Range. In any weather, the frequent landslides on Highway 37 obstruct the free flow of traffic. People and infrastructure may be put at risk because of the unpredictability of rockfall events' frequency and size (Dorren 2003). Natural slopes become more vulnerable to failures when converted into cut slopes by human intervention for the purpose of transportation work, construction of dams, bridges, tunnels and other civil engineering structures (Vishal et al. 2010; Das et al. 2010). In the wet season, Nungkao road cut slope is particularly fragile and often suffers from rock falls. A number of hanging blocks have been discovered on site slopes as a result of blasting and mechanical excavation. The area is vulnerable to collapse because of the steep slope of the road. Geomechanical classification of the rock mass (Bieniawski 1979) was also used, with the application of a rock mass rating (RMR) system (Bieniawski 1974, 1975, 1976, 1989). RMR is a rating-based classification method in which ratings have been given to different parameters influencing the stability of rock mass, and their algebraic sum defines the quality of rock mass.The methodologies applied are obviously simple but an effective ways to describe the potential behaviour of the rock mass with respect to the probability of occurrence of slope movements. A greater knowledge of the variables that lead to landslides may help reduce the risk of rockslides. Rock mass rating (RMR) is a useful tool in describing rock masses among the several approaches for identifying rock masses. The RMR method is used to examine the strength of the exposed rocks on the slope face, the spacing and direction of discontinuities, and the conditions of groundwater. Generally, a landslide study aims to interpret the safety factor of either or both the soil and rock slopes by applying the most feasible and reliable techniques from the available resources.

7.2 Study Area

The Barak basin is a crucial element of the Indo-Myanmar orogenic belts. The Nungkao Landslide is located at 24º46´29.00˝N and 93º18´45.00˝E on toposheet No. 83 H/5 of the Survey of India. The landslide is located at an elevation of 264 m above sea level, around 138.6 kms from Imphal, the capital city (Fig. 7.1). It is located at Tamenglong district of Manipur along Imphal-Jiribam National Highway 37.

The rock exposure in the present study area belongs to the Surma group of rocks (Fig. 7.2). It occupies most of the western hills of the state, Manipur. Surmas are considered as the molasse deposits, which are well developed in Mizoram and have its extension up to Manipur and Nagaland.

Intercalations of light grey, fine to medium grain; thickly bedded, massive sandstones and dark grey, fine-grained; laminated to thinly bedded shale and siltstone form this group. Sandstone from Surma is composed of quartz, lithic pieces (plagioclase), and K-feldspar. The block size varies widely across slopes, resulting in irregular rock falls. Despite the fact that mechanical excavation has caused the parallel bedding joints to lose their continuity, their persistence has been substantially decreased. The

Fig. 7.1 Slope section of Nungkao Landslide showing variable block size due to uncontrolled blasting

most common method of detaching a wedge is not by sliding it along the junction line but rather by causing it to fall naturally. The other causes of the landslide are structural features and lithological parameters, which are aggravated by anthropological and other factors. An attempt has been made to interpret the nature of the slide/fall in the area.

7.3 Methodology

The methodology designed for this study is to identify potential points of failure in the region. To begin with, a geotechnical examination on soil and rock is carried out. Further, combined data (persistence, spacing, aperture, and infilling) are analysed. Using RMR and failure mode analysis, SMR values shall be obtained for each block. The steps in the process are described in detail in the sections that follow.

7.3.1 Geotechnical Approach

In order to determine the strength of the slope-forming rocks and soils, a study on mechanical strength is essential in landslide investigation. The mechanical strength of rock and soil may be evaluated using a variety of techniques. The characteristics of rock strength in uniaxial compression (C_o), in tension (T), and in shear (τ) are widely used parameters of rock mechanics. Uniaxial compression and Brazilian

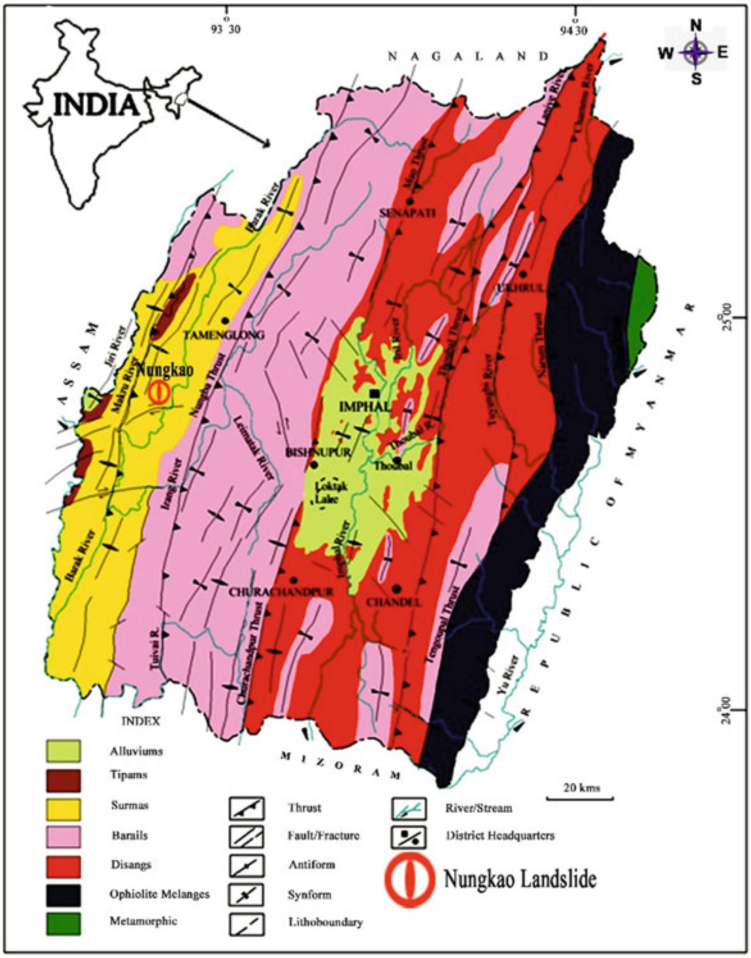

Fig. 7.2 Geological map of Manipur showing Nungkao landslide

tests are used in this investigation to evaluate the unconfined compressive and tensile strengths of rocks from the Surma group in the study region. The "Core Drilling Machine" is used to cut samples perpendicular and parallel to the bedding. Samples of a cylindrical core with a length-to-diameter ratio of 2:1 and 1:1 were obtained for the Compressive and Brazilian tests.

Compressive Strength International Society for Rock Mechanics (ISRM) recommends a standard approach for evaluating the compressive strength of rock with a 42 ± 3 mm diameter cylindrical sample. Four samples, each one parallel to and perpendicular to bedding, have been tested and it is represented by relationship

$$C_0 = C_s(0.8 + 0.2/D) \tag{7.1}$$

Table 7.1 Mean Uniaxial Compressive strength (UCS)

Rock sample nature	Load (P) in kN	Mean diameter (cm)	Radius (cm)	Compressive strength $C_0 = P/A(P/\pi r^2)$ in MPa
Parallel	55.04	3.29	1.65	64.75
Perpendicular	77	3.308	1.655	89.75
Mean	66.02	3.3	1.65	77.25

where, C_0 is the observed compressive strength, D is the diameter of the specimen for which $2 > D > 1/3$ is assumed, C_s is regarded as the standard compressive (uniaxial) strength (at least three tests conducted).

Generally, the uniaxial compressive strength, C_0 is given by

$$C_0 = P/A \tag{7.2}$$

where, P = applied load, A = cross-sectional area of the sample. Uniaxial compressive strength is determined for the Surma sandstones parallel and perpendicular to bedding, and the results are shown in Table 7.1.

Tensile Strength It is also called Brazilian Test. The same compressive machine is used in this test. When the compressive force is applied to the sample, it fails due to tension. So, tensile strength is given by

$$T_b = 2P/\pi DL; \tag{7.3}$$

where P stands for the applied force, D for the sample diameter, and L for the sample length

The International Society for Rock Mechanics (ISRM) recommends a 54-mm diameter, a 200-N-per-second stress rate, and a 200-N-per-second tensile strength (ISRM 1981):

$$T_b = 0.636P/DL; \tag{7.4}$$

where P stands for the applied force, D for the sample diameter, and L for the sample length. Tensile strength determined by the Brazilian test is presented in Table 7.2.

Failure Envelope

Table 7.2 Mean tensile strength

Rock sample nature	Load (P) in kN	Mean diameter (cm)	Mean length (cm)	Tensile strength $T = 2P/\pi DL$(MPa)
Perpendicular	13.96	3.32	3.48	8
Parallel	11.625	3.321	3.4375	6.5
Mean	12.79	3.32	3.43	7.25

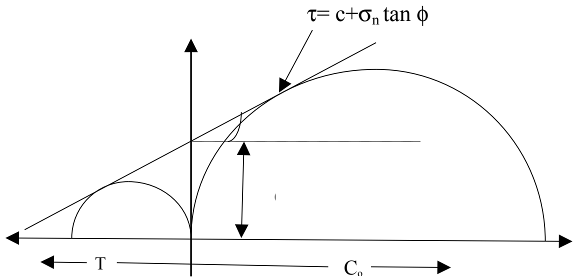

Fig. 7.3 Mohr's failure envelope

Table 7.3 Strength parameters of samples

Rock sample	Cohesion C (MPa)	Internal friction angle, ϕ	Normal stress σ_n (MPa)	Shear strength $\tau = C + \sigma_n \tan\phi$ (MPa)
Perpendicular	12.65	55.75	5.25	23.14
Parallel	9.00	53.87	6.37	17.72
Mean	10.81	54.81	5.81	20.43

Mohr's stress circle, which displays compressive strength values to the right of zero on the circle, can be used to display the results of these tests.

Tensile strength is to the left of zero on the horizontal axis. The diameter of the circles is determined by the uniaxial compressive and tensile strength factors (Fig. 7.3). Figure 7.3 shows a common tangent created between the two circles. When the Y-axis or Shear Stress τ-axis (Y) is intersected with this line, the value of cohesion, C, is calculated. The magnitude of normal stress is given by the point where this tangent intersects the right circle, σ_n (along the x-axis). The failure envelope may be calculated using the formula $\tau = C + \sigma_n \tan\boldsymbol{\phi}$, i.e., its shear strength parameters(Table 7.3).

As a result, an average UCS of 77.25 MPa is used for slope stability study of RMR and SMR rock.

Kinematic Analysis Discontinuities data are collected from the field to analyse various slope failure modes. Rockpack III software is used to establish the mode of slope collapses. The discontinuity data collected from the field is analysed and aggregated in a scientific manner (Fig. 7.4).

The intersecting line of discontinuity planes is found in the shadow zone, with a 60°/092° dip, using Rockpack III. The most common type of landslide collapse is wedge failure. During a wedge failure, the slope face's dip angle is less than the line of discontinuity's plunge angle (Markland test). Researchers Markland (1972), Hocking (1976), Cruden (1978), Goodman (1976), Hoek and Bray (1981), Lucas (1980), Matherson (1988), Yoon et al. (2002) and Saranaathan and Kannan (2017) have used this strategy. The probability of failure and the mode of failure are determined using discontinuity-slope surface connections (Kliche 1999). Technically, the breakdown was caused by a wedge failure (Fig. 7.4).

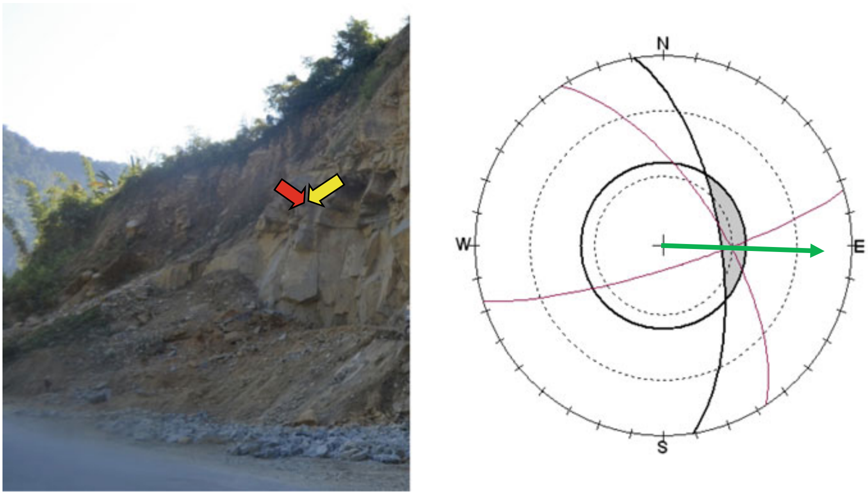

(a) (b)

Fig. 7.4 **a** Field photograph and **b** Stereoplot showing probable mode of Wedge failure

7.3.2 Rock Mass Rating (RMR)

The modified RMR (Bieniawski 1979) utilizes the first five parameters, namely rock strength (RQD), spacing of discontinuities (discontinuity conditions), and groundwater conditions, to classify rock masses (and discontinuity orientation). All the ratings are algebraically summarized and can be adjusted with discontinuity orientation as shown in the following equations, and the values so obtained are shown in Tables 7.4, 7.5, and 7.6.

$$\text{RMR} = \text{RMR}_{basic} + \text{ adjustment of discontinuity orientation} \tag{7.5}$$

$$\text{RMR}_{basic} = \sum \text{parameters } (\text{i} + \text{ii} + \text{iii} + \text{iv} + \text{v}) \tag{7.6}$$

Table 7.4 Slope characteristics and Strength Parameters of the Landslide area

Station	Location	Attitude of slope (°)	Type of Rock	Discontinuity attitude (°)	Degree of weathering	Strength
						Qc (MPa)
Nungkao	24º46´29.00˝N 93º18´45.00˝E	65/081	Massive to thickly bedded sandstone	66/057 80/163	Low	77.25

Table 7.5 Orientation of Discontinuities and Slopes

Station	Aj	Bj	As	Bs	Aj–As	Bj + Bs−180	Probable failure
Nungkao	98	81	81	65	17	34	Wedge

Table 7.6 RMR Determination

Station	Strength	RQD	Spacing	jL	jR	jA	jC	Ground water	RMR
Nungkao	7	17	15	2	2	1	4	15	58

jL = joint continuity or length, jR = joint roughness, jA = joint alteration, jC = joint condition factor

The algebraic sum of the parameters is the numerical value of RMR. It is indicated that the RMR value belongs to the fair rock category of class III. Slope mass rating (SMR) is a modified form of Bieniawski's rock mass rating used to evaluate slope stability. To overcome the shortcomings of RMR, Romana (1993) suggested the SMR system, which includes adjustment factors (F_1, F_2, and F_3) in RMR. Finally, Eq. (7.7) can be used to calculate SMR (Romana 1985, 1993; Romana et al. 2003).

$$\mathbf{SMR} = \mathbf{RMR}_b + (\mathbf{F_1} \times \mathbf{F_2} \times \mathbf{F_3}) + \mathbf{F_4} \tag{7.7}$$

Bieniawski rock mass classification RMR index is $\mathbf{F_1}$ is the parallelism between discontinuity dip direction and slope dip; $\mathbf{F_2}$ is the discontinuity dip; $\mathbf{F_3}$ is the slope-discontinuity connection, and $\mathbf{F_4}$ is a correction factor that varies based on the excavation method**.** The value obtained from the addition of adjustment factors is then summed up with RMR_B in order to get the total SMR value (Table 7.7).

Due to the modified SMR study's inability to show the factor of safety (F) instability's full extent, a stability analysis based on Hoek and Bray (1981) wedge failure calculation may be used.

7.3.2.1 Calculation of Factor of Safety (F) for Wedge Failure

In the present study, the calculation of the factor of safety (F) is governed by Hoek and Bray's (1981) method. In the mode of failure, planar, wedge, and toppling are considered. Wedge failure is observed and accordingly makes an attempt to interpret safety factors. For **wedge** failure, the following formula is utilized

$$F = \frac{3}{\gamma H}(C_A.X + C_B.Y) + \left(A - \frac{\gamma_\omega}{2\gamma}.X\right)\mathrm{Tan}\varnothing_A + \left(B - \frac{\gamma_\omega}{2\gamma}.Y\right)\mathrm{Tan}\varnothing_B$$

where, C_A and C_B are the cohesion of the planes A and B.

Φ_A and Φ_B are the angles of friction on joint/weak/discontinuities planes A and B, respectively

Table 7.7 Calculation of SMR and stability classes

Station	RMR	Rating for adjustment factor				SMR	CLASS	Description	Stability	Failure	Support
		F_1	F_2	F_3	F_4						
Nungkao	58	0.7	1.0	−25	0	41	III	Normal	Partially Stable	Some joints or many wedges	Systematic

Table 7.8 Result of soil test for Nungkao

Moisture content	Specific gravity	Plastic limit	Liquid limit	Shrinkage limit	Plasticity index	Liquidity index	Consistency index
12.91	2.6	22.02	26.5	30.22	4.48	−1.18	3.03

Table 7.9 Values of Liquidity Index (I_L) and Consistency Index (I_C) to consistency of soil (Murthy, 2007)

Consistency	Liquidity Index (I_L)	Consistency Index (I_C)
Semi-solid or Solid State	Negative	>1
Very stiff state	0	1
Very soft state	1	0
Liquid State(when disturbed)	>1	Negative

γ is the unit weight of the rock in g/cc, γ_ω is the unit weight of water in g/cc, and H is the total height of the wedge in cm

X, Y, A, and B are dimensionless factors that depend upon the geometry of the wedge

$X = \mathrm{Sin}\theta_{24} / \mathrm{Sin}\theta_{45}.\mathrm{Cos}2_{na}$

$Y = \mathrm{Sin}\theta_{13} / \mathrm{Sin}\theta_{35}.\mathrm{Cos}1_{nb}$

$A = \mathrm{Cos}\psi_a - \mathrm{Cos}\psi_b.\mathrm{Cos}\theta_{na.nb} / \mathrm{Sin}\psi_5.\mathrm{Sin}2\theta_{na.nb}$

$B = \mathrm{Cos}\psi_b - \mathrm{Cos}\psi a.\mathrm{Cos}\theta_{na.nb} / \mathrm{Sin}\psi 5.\mathrm{Sin}2\theta_{na.nb}$,

where, ψ_a and ψ_b are the dips of planes A and B, respectively, and ψ_5 is the dip of intersection.

7.3.2.2 Study of Soil Properties

In landslide investigation, it is essential to understand the characteristics of soil morphology. Laboratory analysis of soil samples was done, and the results are presented in Tables 7.8 and 7.9.

The soil samples fall into the inorganic clay group on the plasticity index chart, suggesting a more inorganic soil composition. Consequently, the (−ve) liquidity index (**−1.18**) and the (+ve) consistency index (**3.03**) suggest that the slope-forming materials exist as solid or semi-solid material.

7.3.2.3 Shear Strength

Landslides and foundation failures may occur if the soil does not have the ability to withstand such shear loads (Liu and Evett 1981). Soil gains its shear strength from its internal friction angle and cohesion and can be measured using the Coulomb's equation,

Table 7.10 Normal stress and shear stress parameters of soils of Nungkao Landslide area

Sample No.	σ (kN/m^2)	τ (kN/m^2)
S-1	9.8	3.1
S-2	19.6	4.7
S-3	29.4	6.96

$$t = c + \sigma_n \mathrm{Tan}\phi \tag{7.8}$$

where, c = cohesion, σ_n = Normal stress and ϕ = Internal friction angle.

Three soil samples were taken for direct shear test in the laboratory, and the results are shown in Table 7.10.

The shear strength parameter of the soil is determined as
Cohesion, c = 1 kN/m^2 and
Internal friction angle, ϕ = 20°.

7.3.2.4 Calculation of Factor of Safety for Soil

$$\text{Slope angle} = 65^\circ \quad \text{Cohesion, c} = 1\ \mathrm{kN/m^2} = 1{,}000\ \mathrm{N/m^2}$$
$$\text{Internal friction angle, } \phi = 20^\circ \quad \tan\phi = \tan 20^\circ = 0.36397$$
$$\text{Slope height, H} = 75\ \mathrm{m} \quad \text{Unit weight, } \gamma = 0.2548\ \mathrm{kN/m^3} = 254.8\ \mathrm{N/m^3}$$

Now we get,

$$\frac{c}{\gamma \cdot \mathrm{H} \cdot \mathrm{Tan}\phi} = \frac{1000}{254.8 \times 75 \times 0.36397} = 0.1438$$

Again, from the Chart 2 (after Hoek and Bray 1981), corresponding to this value which intersects slope angle (20°),

$$\frac{\mathrm{Tan}\phi}{F} = 0.28$$

$$\Rightarrow F = \frac{0.36397}{0.28} = 1.3$$

As a result, the slope of Nungkao has a factor of safety of 1.3, which is greater than 1, and so falls under the stable slope criterion.

7.4 Results and Discussion

Prepared core samples which are perpendicular to bedding showed higher compressive strength than those taken parallel to bedding, suggesting the presence of structurally weak planes or surfaces, as well as other irregularities that are almost invisible to the naked eye. The main type of rocks comprises the intercalations of Sandstones and Shales, where the outcrop exhibits near horizontal bedding and many joint sets. Block/wedge failure results from a succession of varying-sized wedges formed by the intersection of joint planes with respect to the slope angle. In Table 7.11 (Slope Stabilization), the Rock Mass Rating value is 58, which is in the fair category of class III (Table 7.12).

After a thorough investigation of the soil it is inferred that the factor of safety for soil has 1.3, suggesting stable condition. The soil cover at slopes is very thin, and therefore, it may not cause any kind of major landslide. A small stream of first-order runs near the area which may bring changes in the hydrostatic condition of the site by increasing its weight after getting saturated with water during the rainy season. In addition, anthropogenic activity such as a faulty road cut design and an incorrect blasting technique might have triggered the slip and fall.

7.4.1 Wedge Failure Safety Factor Calculation

See (Table 7.13).

Two Prominent joint planes are mainly responsible for the failure of this slope which is clearly revealed through kinematic analysis (Fig. 7.4), and consequent analysis interpret the factor of safety following the Hoek and Brown wedge failure technique using stereo plot (Fig. 7.5). From the analysis it shows that the wedge failure analysis through stereo-net, the plunge of the two intersections is 60º and its direction of movement is at N92. The safety factor is greater than 1, indicating stable

Table 7.11 Description of SMR classes (Romana, 1985)

CLASS	III
SMR	41
DESCRIPTION	Fair
STABILITY	Partially stable
FAILURE	Some joints or many Wedges
SUPPORT	Systematic

Table 7.12 Support for SMR Classes (Romana, 1985)

SMR CLASS	Support	Description
III	Systematic	Systematic bolting, dental treatment, bolting, net toe drains

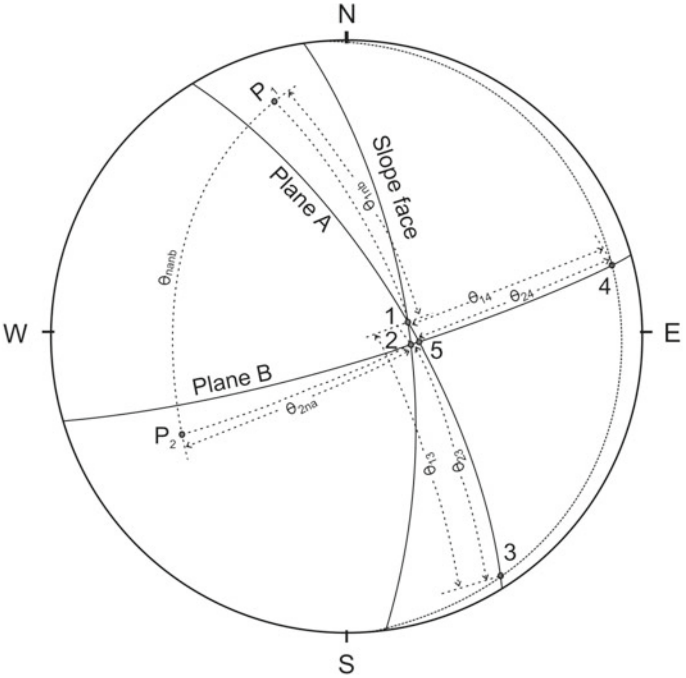

Fig. 7.5 Stereo-plot of data for wedge stability analysis

Table 7.13 Wedge analysis calculation (Hoek and Bray, 1981)

Inputs	Values	Calculation
$\psi_a = 66°$ $\psi_b = 80°$ $\psi_5 = 60°$ $\theta_{na.nb} = 96°$	$\text{Cos } \psi_a = 0.407$ $\text{Cos } \psi_b = 0.407$ $\text{Sin } \psi 5 = 0.866$ $\text{Cos } \theta_{na.nb} = -0.105$ $\text{Sin } \theta_{na.nb} = 0.995$	$A = \frac{cos\psi a - cos\psi b.cos\theta na.nb}{sin\varphi_5.sin^2\theta na.nb} = 0.524$ $B = \frac{cos\psi b - cos\psi a.cos\theta na.nb}{sin\varphi_5.sin^2\theta na.nb} = 0.522$
$\theta_{24} = 51°$ $\theta_{45} = 48°$ $\theta_{2na} = 79°$ $\theta_{13} = 75°$ $\theta_{35} = 66°$ $\theta_{1nb} = 80°$	$\text{Sin } \theta_{24} = 0.777$ $\text{Sin } \theta_{48} = 0.743$ $\text{Cos } \theta_{2na} = 0.191$ $\text{Sin } \theta_{13} = 0.966$ $\text{Sin } \theta_{35} = 0914$ $\text{Cos } \theta_{1nb} = 0.174$	$X = \frac{Sin\theta_{24}}{Sin\theta_{45}Cos\theta_{2na}} = 5.481$ $Y = \frac{Sin\theta_{13}}{Sin\theta_{35}Cos\theta_{1nb}} = 6.089$
$\Phi_A = 55°$ $\Phi_{\mathbf{B}} = 55°$ $\gamma = 2.65$ g/cc $\gamma_\omega = 1$ g/cc $C_A = 1{,}080$ g/cc $C_B = 1{,}080$ g/cc $H = 1{,}600$ cm	$\text{Tan } \Phi_A = 1.428$ $\text{Tan } \Phi_B = 1.428$ $\gamma = 2.65$ $\gamma_\omega/2\gamma = 0.1885$ $3C_A/\gamma H = 0.763$ $3C_B/\gamma H = 0.763$	$F = 3\frac{C_A}{\gamma H}.X + 3\frac{C_B}{\gamma H}.Y + \left(A - \frac{\gamma_\omega}{2\gamma}.X\right)Tan\varnothing_A + \left(B - \frac{\gamma_\omega}{2\gamma}.Y\right)Tan\bullet\varnothing_B = 7.2105$

condition. Both soil and rock revealed the stable condition of the study area, but the site has been affected by recurrent slides in almost all the rainy season, either as rock fall or as soil slides and sometimes together.

7.4.2 *Preventive Measures*

Some loose and dangling blocks have been uncovered on the slopes after an incorrect blasting procedure. A steel wire net must be installed to support the weight of the blocks and prevent them from collapsing into the streets. A popular way to stabilise slopes by minimising movement-inducing stresses is to remove any unstable or potentially unstable blocks. Another measure to be adopted in this site is to reduce the slope angle of the road cut. With respect to the slope height, it is necessary to have at least two benches so that the rock falling from a great height cannot directly hit the road, which is highly dangerous during heavy vehicular traffic movement. Benches at a minimum width of 2.5 m and drainage ditches to remove water away from the slope are highly recommended. Thus the site needs to have a proper drainage facility, otherwise, percolation of rain or surface water through the weak planes can cause weakening of the shear strength of rocks, thereby initiating sliding/falling of rock blocks.

7.5 Conclusions

Using RMR and SMR, the current research area offers information on the nature of the rock mass as a whole. The failure of the wedge is confirmed by a kinematic examination of the region. A stereographic analysis utilising Rock pack III software detected the various types of slope failure by methodically processing and tabulating discontinuity data acquired from the field. There is a strong likelihood that the landslide will fall as a wedge if its joints (J1 and J2) are located in the shadow region, where the intersecting lines of discontinuity are 60°/092°. According to the plasticity index chart, soil samples taken from site slopes have lower moisture content, which indicates that the soil is of an inorganic origin. As a result, the slope-forming materials are solid or semi-solid, as indicated by the (−ve) value of the fluidity index (−1.18) and the (+ve) value of the consistency index (3.03). As a result, the rock mass along NH 37's slopes is only partially stable. Both rock and soil analyses indicate a stable condition of the study area; however, still a major threat to vehicular movement in this area due to the frequent slides almost every year.

References

Bieniawski ZT (1973) Engineering classification of jointed rock masses. CivEng South Afr 15:335–344

Bieniawski ZT (1974) Geomechanics classification in rock massesand its application in tunnelling. In: Advances in rock mechanics, Proc of 3rd congress of ISRM, National Academy of Sciences, Washington, D.C., II (A), pp 27–32

Bieniawski ZT (1975) Case studies: prediction of rock mass behaviour by geomechanics classification. In: Proceedings of 2nd Australia–New Zealand conference geomechanics, Brisbane, pp 36–41

Bieniawski ZT (1976) Rock mass classifications in engineering. In: Proceedings of the symposium on exploration rock engineering, Johannesburg, pp 97–106

Bieniawski ZT (1979) The Geomechanics classification in rock engineering applications. In: Proceedings of the 4th congress of the international society of rock mechanics, Montreux, Switzerland, vol 2. AA Balkema, Rotterdam, pp 41–80

Bieniawski ZT (1989) Engineering rock mass classification. Wiley, New York, p 251

Cruden DM (1978) Discussion of Hocking's paper "A method for distinguishing between single and double plane sliding of tetrahedral wedges". Int J Rock Mech Mining Sci Geomech Abstr 15(4):217–217

Das I, Sahoo S, Van Weston C, Stein A, Hack R (2010) Landslide susceptibility assessment using logistic regression and its comparison with a rock mass classification system, along a road section in the northern Himalayas (India). Geomorphology 114:627–637

Dorren L (2003) A review of rockfall mechanics and modelling approaches. Prog Physgeogr 27(1):68–87

Goodman RE (1976) Methods of geological engineering in discontinuous rocks. West Publishing, San Francisco

Hocking G (1976) A method for distinguishing between single and double plane sliding of tetrahedral wedges. Int J Rock Mech Min Sci Geomech Abstr 13(7):225–226

Hoek E, Bray JW (1981) Rock slope engineering, 3rd edn. Institution of Mining and Metallurgy, London, pp 57, 92, 96, 150, 358

ISRM (1981) Rock characterisation testing and monitoring. In: Brown ET (ed) Pergamon Press, Oxford

Kliche CA (1999) Rock slope stability. SME, Littleton, CO

Liu C, Evett JB (1981) Soils and foundations. Prentice Hall, INC., Englewood Cliffs, New Jersey 07632, p 28

Lucas JM (1980) A general stereographic method for determining possible mode of failure of any tetrahedral rock wedge. Int J Rock Mech Min Sci Geomech Abstr 17:57–61

Markland JT (1972) A useful technique for estimating the stability of rock slopes when the rigid wedge sliding type of failure is expected. Imp Coll Rock Mech Res Rep, pp 10, 19

Matherson GD (1988) The collection and use of field discontinuity data in rock slope design. Q J Eng Geol 22:19–30

Murthy VNS (2007) Soil mechanics and foundation engineering, geotechnical engineering series, 1st ed. In: Satish Kumar J (ed) CBS Publisher & Distributor, New Delhi, pp 81–119.

Romana M (1985) A geomechanical classification for slopes: slope mass rating. In: Hudson JA (ed) Comprehensive Rock Eng. Pergamon Press, London, pp 375–601

Romana M (1993) SMR classification. In: Romana M (ed) Proceeding of the 7th ISRM international congress on rock mechanics, Achen, 16–20 September 1991, vol 2. A.A. Balkema, Rotterdam, pp 955-960; 1991. Int J Rock Mech Mining Sci Geomech Abstr 30:A231–A231

Romana M, Seron JB, Montlar E (2003) SMR geomechanics classification: application, experience and validation. In: Merwe JN (ed) Proceedings of the 10th congress of the international society for rock mechanics. ISRM 2003-technology roadmap for rock mechanics. SouthAfrican Institute of Mining and Metallurgy, pp 1–4.

Saranaathan SE, Kannan M (2017) SMR and kinematic analysis for slope instability along bodi-bodimettu ghat section, Tamil Nadu. Geol Soc India 89:589–599

Vishal V, Pradhan SP, Singh TN (2010) Instability assessment of mine slope—a finite element approach. Int J Earth Sci Eng 3(6):11–23

Yoon WS, Jeong U, Choi JW, Kim JH, Kim WY, Kim CS (2002) Slope failure index system based on the behaviour characteristics, SFi–system. J Kor Geotech Soc 18:23–37